



Rescue and quality control of historical geomagnetic measurement at Sheshan observatory, China

Suqin Zhang¹, Changhua Fu¹, Jianjun Wang², Guohao Zhu³, Chuanhua Chen⁴, Shaopeng He⁵, Pengkun Guo⁵, and Guoping Chang⁵

¹Institute of Geophysics, China Earthquake Administration, Beijing, 100081, China

²Earthquake Administration of Gansu Province, Lanzhou, 730000, China

³Shanghai Earthquake Agency, Shanghai, 200062, China

⁴Earthquake Administration of Shandong Province, Jinan, 250014, China

⁵Hebei Earthquake Agency, Hebei Province, Shijiazhuang, 050022, China

Correspondence: Changhua Fu (pangzhayu@139.com)

Received: 12 June 2022 – Discussion started: 27 June 2022

Revised: 29 August 2022 – Accepted: 31 October 2022 – Published: 24 November 2022

Abstract. The Sheshan Geomagnetic Observatory (International Association of Geomagnetism and Aeronomy (IAGA) code SSH), China was built in Xujiahui, Shanghai in 1874 and moved to Sheshan, Shanghai at the end of 1932. So far, the SSH has a history of nearly 150 years. It is one of the earliest geomagnetic observatories in China and one of the geomagnetic observatories with the longest history in the world. In this paper, we present the rescue and quality control (QC) of the historical data at the SSH from 1933 to 2019. The rescued data are the absolute hourly mean values (AHMVs) of declination (D), horizontal (H), and vertical (Z) components. Some of these data are paper-based records and some are stored in a floppy disk in BAS, DBF, MDB, and other file storage formats. After digitization and format transformation, we imported the data into the Toad database to achieve the unified data management. We performed statistics of completeness, visual analysis, outliers detects, and data correction on the stored data. We then conducted the consistency test of daily variation and secular variation (SV) by comparing the corrected data with the data of the reference observatory, and the computational data of the COV-OBS model, respectively. The consistency test reveals good agreement. However, the individual data should be used with caution because these data are suspicious values, but there is not any explanation or change registered in the available metadata and logbooks. Finally, we present examples of the datasets in discriminating geomagnetic jerks and study of storms. The digitized and quality-controlled AHMVs data are available at: <https://doi.org/10.5281/zenodo.7005471> (Zhang et al., 2022).

1 Introduction

Geomagnetic observation data contains abundant solar–terrestrial spatial information, which is widely used in geoscience and space science research. The observation data with time resolutions of 1 s to 1 h are usually used to study various short-period magnetic events such as pulsation, geomagnetic crochet, geomagnetic bay, and magnetic storm (Zhao et al., 2019), and to monitor and predict the electromagnetic environment in solar–terrestrial space. At the same time, it also has important applications in detecting underground electrical structures and evaluating the impact of ge-

omagnetic induced current (GIC) on underground metal pipe network, transmission network, communication cables, high-speed railway lines, and other major projects (Kappenman, 1996; Bolduc et al., 1998, 2002; Boteler et al., 1998; Liu et al., 2008, 2016; Liu et al., 2009; Guo et al., 2015). Observation data with time resolution of 1 h to hundreds of years are usually used for the study of the geomagnetic field and its secular variation (SV), such as geomagnetic jerk (Courtillot and Mouël, 1984; Xu, 2009), magnetic pole movement, dipole magnetic moment change, westward drift, etc., which

are of great significance for understanding the material flow inside the core and at the core mantle boundary.

The development and application of geomagnetism depends on long-term data accumulation. The long-term operation of the geomagnetic observatory is very important for the study of the geomagnetic field (Linthe et al., 2013). It is especially valuable to study the variation characteristics of the geomagnetic field from decades to hundreds of years (Clarke et al., 2009; Zhang et al., 2008b). Using the latest scientific and technological means to analyze the continuous geomagnetic observation data as long as possible, to obtain the variation information of the geomagnetic field, has always been a method often used by scientific researchers. However, not all data can be directly provided to researchers, because some data still exist only in the form of hard copy, and even some data face the risk of serious damage and loss due to improper storage conditions. Therefore, it is very important to rescue and digitize these data as soon as possible. High-quality data are the basis of scientific research and the prerequisite for obtaining valuable results (Linthe et al., 2013). Scientists around the world have paid more and more attention to the accumulation of observation data, the rescue of historical data and the sharing of scientific data resources (Curto and Marsal., 2007; Peng et al., 2007; Chulliat et al., 2009; Korte et al., 2009; Dawson et al., 2009; Reay et al., 2013; Morozova et al., 2014, 2021; Sergeeva et al., 2021; Dong et al., 2009; Zhao et al., 2017; Thomson, 2020).

The rescue, recovery, digitization, and the quality control (QC) of historical geomagnetic data are of extraordinary importance for the geomagnetic community (Rasson et al., 2011). This paper presents the collection, collation, digitization, quality control, and correction of the historical data of the Sheshan Geomagnetic Observatory (International Association of Geomagnetism and Aeronomy code SSH) from 1933 to 2019. The SSH Geomagnetic Observatory is the geomagnetic observatory with the longest history in China. Although many efforts have been made (Gao and Hu, 1993), the existing data are still insufficient. Our work aims at filling the lack of observation data at the SSH observatory since 1933, presenting the data of absolute hourly mean values (AHMVs) collected from 1933 to 2019.

This paper is organized as follows. Section 2 describes the data acquisition method, providing information about SSH observatory history, data sources, and the digitization method. Section 3 introduces the quality control of the digitized data. Section 4 describes the correction of the selected problem data. Section 5 describes the validation of the corrected series by comparing it with reference series and Sect. 6 presents application examples of the datasets. Concluding remarks are given in Sect. 7.

2 Data production methods

2.1 The Sheshan geomagnetic observatory

The first step of the data-rescue process was to collect resources scattered in different locations, which exist in various forms, including data and metadata that may have an influence on data rescue (observatory relocation, instrument replacement, replacement of observers, environmental change, etc.). We have carefully examined the documentation stored in the SSH, Geomagnetic Network of China (GNC), and reference room of the Institute of Geophysics, China Earthquake Administration (IGPCEA). The reference room is a resource center of the IGPCEA, used to collect books, journals, papers, monographs, unpublished reports, internal textbooks, research reports, reference documents, and scientific research achievements related to the discipline. It took us nearly 2 months to collect resources. The documentation consulted includes the *Observatory Communication Journal*, *Geomagnetic Observation Report*, *Chronicles of China Geomagnetic Observatory*, and postal letters. The metadata are mainly stored in the *Chronicles of China Geomagnetic Observatory* and the *Geomagnetic Observation Report*. An example of the cover of the bibliographic documents is shown in Fig. 1. The data of 1933–1954 were recorded in the *Geomagnetic Observation Report*. The observation was interrupted from April 1945 to December 1946 due to World War II. The data of 1955–1994 were stored in the DBF format. The data of 1995–2001 were stored in the BAS format. The data from 2002 to 2006 were stored in the Access database in the MDB format. The DBF, BAS, and MDB are all data file storage formats. The DBF is a tabular data file stored in binary and is the database format used by dBase and Fox-Pro databases in DOS systems. The BAS file format is written in the BASIC language, a plain-text data storage format. The MDB format is a storage format used by Microsoft Access software that can generally be opened directly with ACCESS. The data of 2007, 2008, and 2010 were lost for unknown reasons. The data from August to December 2011, and July to October 2019 were missed due to the failure of absolute observation instruments. Data for other years from 2009 to 2019 are stored in the Oracle database.

The Sheshan Geomagnetic Observatory (SSH) is presently run by IGPCEA and has been in operation for almost 150 years. Its predecessors are the observatory in Xujiahui, Shanghai, and that in Lujiabang, Jiangsu Province. It was established in Xujiahui in 1874 and began continuous geomagnetic observation since then. It was moved from Xujiahui to Lujiabang in 1908 and then from Lujiabang to Sheshan in December 1932. The Sheshan Geomagnetic Observatory is located in Sheshan (latitude: 31.1° N, longitude: 121.2° E), 20 km to the southwest of Shanghai city. The geology of the vicinity of the observatory is Upper Jurassic to Down Cretaceous Andesite. The gradient of the field is about 2–3 nT m⁻¹. The earliest absolute house and recording room

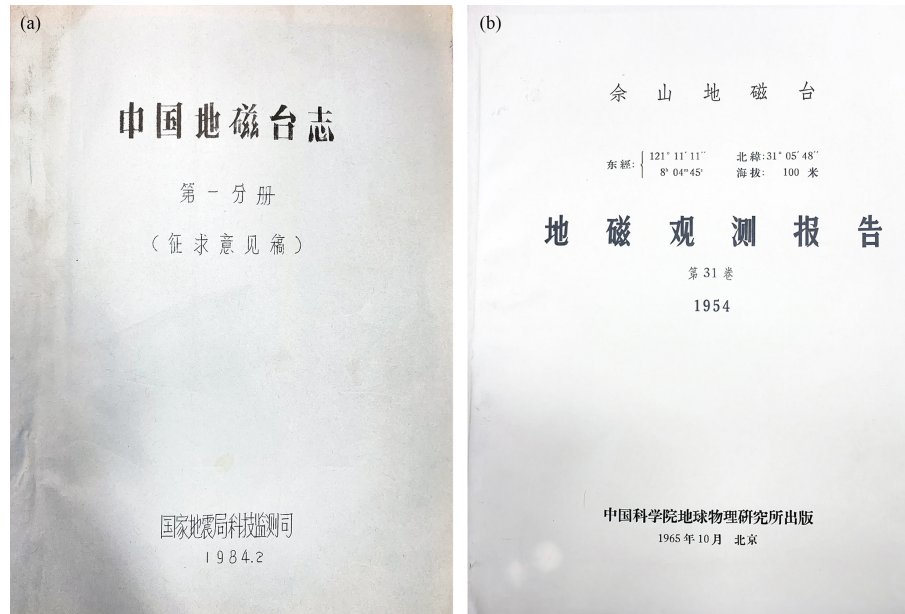


Figure 1. Cover of the (a) *Chronicles of China Geomagnetic Observatory* (Department of Science, Technology and Monitoring, CEA, 1984) and (b) *Geomagnetic Observation Report* (Institute of Geophysics, Chinese Academy of Sciences, 1965).

were built in 1932, they are made of non-magnetic material. The regular observation began in 1933.

Table 1 shows the absolute and relative instruments in the SSH observatory from 1933 to 2019 and the measured geomagnetic elements at different periods. The information was retrieved from the bibliographic documents mentioned above. The first instrument set included an Elliott (D measurement), a Smith (H measurement), and a Schulze (I measurement) as absolute instruments since 1933. The continuous recordings of magnetic variations of declination (D), horizontal (H), and vertical (Z) were obtained respectively with a horizontal variometer (Toepfer) and a vertical intensity variometer (Godhavn) since 1933. Later, a few replacements of instruments took place in the SSH observatory (Table 1). During this period, many jumps were seen in the relative recorded data due to the adjustment of the variometer, the lightning stroke, earthquakes, and other reasons. These jumps have been corrected by the baseline, so that the absolute value is not affected. By 2000, the SSH observatory was equipped with digital instruments. On 1 January 2003, the Schmidt Standard Theodolite was replaced by a DIM-100/353766 Fluxgate Theodolite and an Overhauser Effect Proton Precession Magnetometer GSM-19F replaced the Proton Precession Magnetometer CZM-2.

2.2 Data digitization

Because some records are handwritten or manually mimeographed, it is impossible to automate the digitization process. To facilitate the digitization and further application of these records, all the documents were photographed. It is

also useful for checking the consistency of digitized data and source data in the future. It is not good for old paper copies to be carried around too much and as soon as we have a digital picture, which is fast to make, we can store the respective papers in their normal archive place again with the usual temperature, humidity, etc. Using the character-recognition program to recognize the photos and compare the consistency with the paper data, it was found that the recognition effect of the character was not ideal. It may be due to the light color of the handwriting, or some of the handwriting is fuzzy and unclear. Therefore, the digitization was mainly performed by key input. We digitized the AHMVs of the three components of declination (D), horizontal (H), and vertical (Z). We designed a set of Excel templates to unify the data-entry format. The digital templates are very similar to the original data source to keep track of our work. The input templates include three workbooks, which are used to store the AHMVs of 1 year, including the AHMVs of the D , H , and Z components. Every AHMVs workbook consists of 14 worksheets, including text description, data worksheets from January to December of every year, and automatic summary worksheets. The monthly data worksheet header includes the station code, measuring point ID, date, large value, and 24 hourly mean values. The large value is a fixed value every month. The purpose of entering a large value is to facilitate the rapid entry of each value. The 24 AHMVs can be calculated by adding the large values to the 24 hourly mean values respectively. For example, the large value in January 1985 was 33 300. For each hourly mean value of this month, we only need to input the digits after thousands' digit. If the input value of 0h on 1 January was 146.1, we can get the

Table 1. Summary of instruments in the period from 1933 to 2019 at SSH.

| Component | Absolute measurements | | Relative measurements | |
|-----------|-----------------------|--|-----------------------|---|
| | Date | Instrument name and type | Date | Instrument name and type |
| <i>D</i> | 1933–June 1969 | Magnetometer (Elliott/49) | 1933–2000 | Horizontal variometer (Toepfer) |
| | June 1969–2002 | Standard theodolite (Schmidt/572144) | 2000–2019 | Fluxgate magnetometer (FGE) |
| | 2003–2009 | Fluxgate theodolite (DIM-100/353766) | | |
| | 2009–2019 | Fluxgate theodolite (MINGEO DIM) | | |
| <i>H</i> | 1933–1992 | Magnetometer (Smith/35416) | 1933–2000 | Horizontal variometer (Toepfer) |
| | | | 2000–2019 | Fluxgate magnetometer (FGE) |
| <i>I</i> | 1933–1992 | Geomagnetic induction instrument (Schulze/42) | | |
| | 1993–2009 | Fluxgate theodolite (DIM-100/353766) | | |
| | 2009–2019 | Fluxgate theodolite (MINGEO DIM) | | |
| <i>Z</i> | | | 1933–2000 | Vertical intensity variometer (Godhavn) |
| | | | 2000–2019 | Fluxgate magnetometer (FGE) |
| <i>F</i> | 1981–1985 | Proton precession magnetometer (CHD-5/10) | | |
| | 1985–2002 | Proton precession magnetometer (CZM-2) | | |
| | 2003–2019 | Overhauser effect proton precession magnetometer (GSM-19F) | | |

AHMV at this moment by 33 300 plus 146.1, and so on. Missing values were marked as “99 999”. An example of the Excel tables with digitized data is presented in Fig. 2. The “key input” approach is slower but has the lower error rate (Capozzi et al., 2020). After each month of data entry, we cross checked the digitized data with the original source values in order to identify and remove transcription errors. Using this approach, it took us half a year to digitize the 1933–1954 data from paper records.

2.3 Import data stored in various formats into Oracle database

We developed a data convert software (Fig. 3) to import data stored in various formats (XLS, DBF, BAS, and MDB) into a unified Oracle database. In this way, all AHMVs were stored in the same database in a unified format. We call these stored data without any correction the original AHMVs data; it is convenient for the subsequent analysis and application. This allows us to examine the data using Geomagnetic Data Processing Software (GDPST) developed by the Geomagnetic Network of China (Zhang et al., 2016). The GDPST was developed based on the Oracle database. It provides a convenient way of data processing and comparative analysis. The software also has the functions of the data query, data backup, and data download, etc.

3 Quality control of digitized data of SSH observatory

The purpose of quality control (QC) is to check the completeness and reliability of geomagnetic observation data. The quality of geomagnetic data is often affected by the changes in the instrument or environmental conditions of the measurements, like the repair or re-calibration of the instrument, instrument replacement, observatory relocation, gradual changes of the observation environment, changes in observing process, etc. (Morozova et al., 2014; Zhang et al., 2016). Most such changes can lead to what we call data problems and can be defined as sudden breaks and jumps in the series of geomagnetic data, or gradual biases, or noise and change of transfer function, etc. Correction of problem data before any subsequent analyses is highly desirable (Mestre et al., 2013).

In this study, the QC was performed in order to check the quality of the rescued data. The inspection contents include evaluating the completeness of data, the accuracy of daily variation, the stability of secular variation, and analyzing the influence factors of data quality.

| Large value | 33300 | Station ID 29004 | | | | | | | | | | | | | | | | | Point ID X | | | 1943 | year | 1 | month | 23 |
|-------------|-------|------------------|-------|-------|-------|-------|-------|-------|-------|-------|-------|-------|-------|-------|-------|-------|-------|-------|------------|-------|-------|-------|-------|-------|-------|----|
| date/hour | 0 | 1 | 2 | 3 | 4 | 5 | 6 | 7 | 8 | 9 | 10 | 11 | 12 | 13 | 14 | 15 | 16 | 17 | 18 | 19 | 20 | 21 | 22 | 23 | | |
| 1 | 146.1 | 150.2 | 151.3 | 150.4 | 152.7 | 159.1 | 167.7 | 174.6 | 183.1 | 184.1 | 180.7 | 184.7 | 188.4 | 190.3 | 190 | 184.1 | 181.6 | 171.2 | 165 | 158.2 | 154.1 | 152.3 | 150.9 | 141.1 | | |
| 2 | 146.8 | 152.4 | 151 | 151.6 | 157 | 158.8 | 158.9 | 160.9 | 165.8 | 164.9 | 156.6 | 163.1 | 161.6 | 161.3 | 163.6 | 159.3 | 160.5 | 150.4 | 145.8 | 148.2 | 149.2 | 150.3 | 153.7 | 154.6 | | |
| 3 | 150 | 155.1 | 157.5 | 159.6 | 162.8 | 167.5 | 175.9 | 184.2 | 181.5 | 178.9 | 169.6 | 159.9 | 158.8 | 160.4 | 148.4 | 143.8 | 155.6 | 154.1 | 155.2 | 143.9 | 147.7 | 153 | 153.3 | 158.1 | | |
| 4 | 186.6 | 191.9 | 186.7 | 173.2 | 173.8 | 170.4 | 174.2 | 173.7 | 178.3 | 183.9 | 155.7 | 131.5 | 127.5 | 164.5 | 153 | 141.2 | 131.2 | 172 | 131.1 | 117.9 | 129.5 | 131.5 | 132.6 | 138.3 | | |
| 5 | 126.8 | 136 | 142.5 | 145.3 | 149.9 | 140.1 | 144.9 | 146.5 | 145.9 | 143.7 | 148.6 | 151.1 | 154.3 | 151.4 | 145.2 | 152 | 149.2 | 129.3 | 123.2 | 123.9 | 125.3 | 128.5 | 135.5 | 130.6 | | |
| 6 | 128.9 | 140.6 | 144.8 | 141.6 | 143.3 | 142.8 | 150.7 | 147.8 | 144.5 | 144.6 | 135.3 | 138.5 | 153.1 | 152.9 | 152.7 | 151.8 | 158.1 | 140.3 | 135.5 | 134.1 | 135.9 | 137.7 | 137.7 | 136.9 | | |
| 7 | 140.4 | 149.5 | 149.4 | 148 | 150.5 | 153.1 | 160.3 | 164.3 | 163.5 | 161.6 | 157.8 | 161.3 | 164.4 | 164.2 | 163.5 | 161.4 | 154.5 | 148.1 | 147.5 | 147 | 144.3 | 144.2 | 146.9 | 152.1 | | |
| 8 | 156.7 | 167.6 | 172.8 | 167.9 | 166.1 | 162.7 | 163.6 | 170.8 | 178.3 | 177.8 | 174.8 | 176.8 | 175.4 | 173.1 | 169.9 | 161.5 | 156.7 | 150.7 | 147.8 | 145.6 | 146.4 | 147 | 145.4 | 145.6 | | |
| 9 | 150.6 | 161.4 | 162.7 | 155.4 | 151.8 | 151.4 | 150.5 | 141.8 | 130.8 | 136 | 146.8 | 157.2 | 162.8 | 163.4 | 162 | 159.5 | 154 | 142 | 141.2 | 137.7 | 137.3 | 143 | 143.2 | 144.6 | | |
| 10 | 146.4 | 157.5 | 159.2 | 156.3 | 150.2 | 150.3 | 153.2 | 160.3 | 167.6 | 168.1 | 165 | 169.9 | 167.2 | 165.9 | 163.3 | 162.2 | 156.6 | 151.2 | 148.3 | 142.8 | 139.1 | 140.2 | 146.9 | 143.7 | | |
| 11 | 141.7 | 148.4 | 151.7 | 141.4 | 138.9 | 146.8 | 157.5 | 169.2 | 176.5 | 173.9 | 167.2 | 165.7 | 169.5 | 167.7 | 163.3 | 158.4 | 155.6 | 147.7 | 147.9 | 150 | 146.3 | 152.9 | 158.6 | 160 | | |
| 12 | 170.5 | 175.1 | 171.1 | 169.3 | 168.3 | 175.9 | 165.6 | 170.8 | 170.2 | 163.8 | 161.7 | 164.1 | 169.3 | 165.7 | 164.4 | 164.1 | 161.1 | 149.5 | 144.7 | 144.4 | 143.6 | 148.7 | 150.9 | 152 | | |
| 13 | 151.2 | 156.5 | 152.9 | 146.7 | 146.6 | 150.8 | 157.3 | 165.9 | 169.6 | 173.4 | 167.7 | 165 | 164.1 | 164.5 | 164 | 161.1 | 159 | 153.2 | 149.3 | 148.6 | 149.7 | 152.1 | 149.6 | 151 | | |
| 14 | 152.5 | 157.8 | 156.3 | 149.9 | 151 | 156.4 | 161.4 | 169.3 | 177.1 | 179.7 | 173.7 | 175.5 | 176.9 | 175.2 | 174.2 | 171.9 | 166.7 | 161.2 | 159.4 | 159.1 | 159.1 | 161.3 | 160 | 159.7 | | |
| 15 | 161.9 | 163.6 | 154.7 | 149.5 | 155.8 | 170.6 | 180.3 | 186.5 | 193.1 | 188.8 | 184.8 | 185.4 | 187.4 | 188.3 | 186.8 | 181 | 176.6 | 169.5 | 165 | 161.1 | 158.1 | 160.7 | 161.2 | 162.1 | | |

Figure 2. An example of the Excel tables with digitized data.

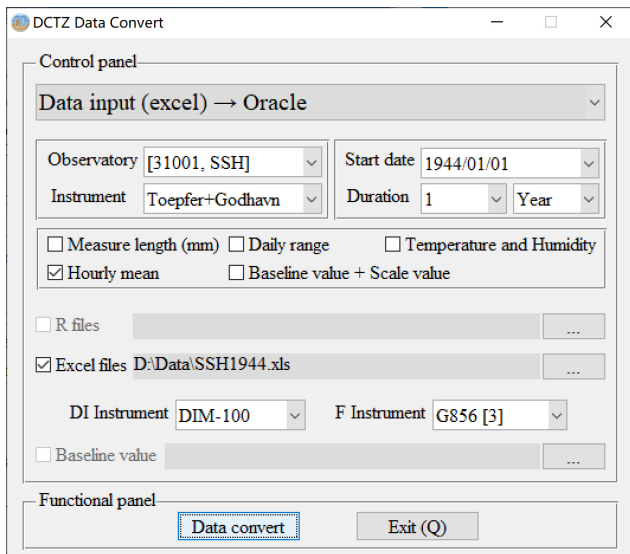


Figure 3. Data import software.

3.1 The completeness of data

Based on the original AHMVs, the annual completeness is calculated using the following Eq. (1):

$$C = (W_e - W_m) / W_e, \tag{1}$$

where C is the completeness of the AHMVs, W_e is the number of expected data in the chosen period, W_m is the number of missing data, see Fig. 4 for the completeness of data. The series in this study consists of data measured from 1933 to 2019. It has 5 larger gaps with a total of 66 months of data missing; the number of missing data accounts for 6.5% of the total. All gaps were not replaced by interpolation in this

study. War and instrument failure are the main reasons for the gaps of observation.

3.2 The accuracy of the rescued data

We have designed a strict quality-control procedure to ensure the accuracy of the rescued data. It consists of the following three steps:

1. *Preliminary analysis of the series, detection of outliers.*
In order to avoid the adverse impact of extreme data on the overall trend, we filtered out clearly obvious outliers by the appropriate filtering function of Excel, such as the missing values which were marked as “99 999”, obvious input error, and so on.
2. *Visual analysis of the series and their first-time derivative (FTD) at different timescales.* After removing the obvious outliers, we plotted AHMVs of the geomagnetic field components D , H , and Z for all time from 1933 to 2019 (see Fig. 5). It can be seen from the figure that the D , H , and Z components have obvious trends. It is the secular variation (SV) in geomagnetic field with time. The additional signal in the plots mainly comes from the activity of external field. The most significant influence is on both the horizontal components D and H ; its influence on the vertical component is minor. In the plots, we do not see obvious step and peak interference.

We checked the AHMV plots of the SSH month by month and found that sometimes the geomagnetic changes were quiet and regular, sometimes violent and irregular, and most of the days the geomagnetic changes were superimposed on the regular quiet day changes with some disturbances of different shapes and amplitude. As shown in Fig. 6, taking the AHMV record of

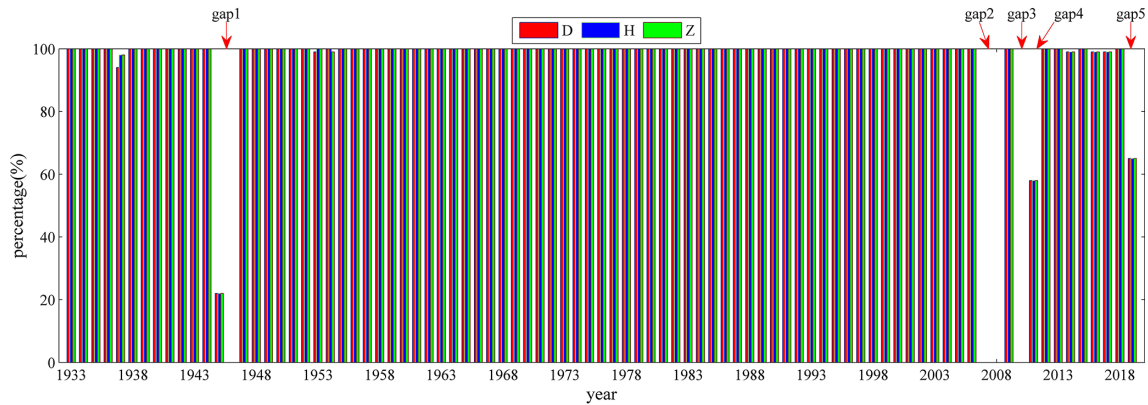


Figure 4. The completeness of the AHMVs from 1933 to 2019.

January 1955 as an example, it can be seen from the figure that the record includes both regular periodic quiet day changes and complex perturbation, and the geomagnetic storms of 18–19 January are violent disturbances.

In order to eliminate the impact of trend and detect the data problems more effectively, we plotted the first-time derivative (FTD) of AHMVs for D , H , and Z components (Fig. 7). We calculated the FTD using the consecutive values of hourly series (Morozova et al., 2014). For all geomagnetic components, the FTD is calculated as

$$dX/dt(\text{hour}) = (X(\text{hour}) - X(\text{hour} - 1))/1, \quad (2)$$

where X denotes the geomagnetic field components D , H , and Z .

The FTD plots are also particularly useful in evaluating artificial noise, especially interference in the shape of steps or spikes (Linthe et al., 2013; Pang et al., 2013; Chen et al., 2014). It can be seen from the figure that the data after the FTD eliminates the trend change, and the data are steady, going up and down within a certain range; ΔD varies between -13.4 and 12.6 min, ΔH varies between -302 and 203 nT, and ΔZ varies between -70 and 62 nT.

3. The tolerance test detects the outliers and compare with geomagnetic indices.

For a large set of data with a normal or approximately normal distribution, 99.7% of the values are distributed in the $(\mu - 3\sigma, \mu + 3\sigma)$ interval, where σ and μ are the standard deviation and mean for all time, respectively. The values beyond this interval are generally considered as outliers. We presented the histograms of the FTD of D , H , and Z components between 1933 and 2019 in Fig. 8, which aimed at detecting the outliers further. The distribution can be well modeled by the Gaussian probability density function (solid red curve). The vertical

dashed red lines indicate the lower and upper limits obtained by applying the criteria $(\mu - 3\sigma)$ and $(\mu + 3\sigma)$. We found that more than 98.6% of the FTD data points fall within the range of 3 times the standard deviations.

For the FTD data exceeding 3 times the standard deviation, we defined them as FTD outliers. We need to confirm whether the outlier is related to geomagnetic activity. Two conventional indices to describe geomagnetic activity are Kp and Dst; Kp has no linear relationship with the geomagnetic activity, so the ap index was introduced. The ap is expressed in “ap units”: 1 ap unit equals 2 nT (Menvielle et al., 2011). Currently, Kp and ap indices are produced by the GeoForschung Zentrum (GFZ) Potsdam, Germany (Kp and ap values since 1932 are available online at <https://www.gfz-potsdam.de/>, last access: 18 November 2022, GeoForschung Zentrum Potsdam Website, 2022); Dst indices are currently produced by the World Data Center for Geomagnetism, Kyoto (Dst values since 1957 are available online at <http://wdc.kugi.kyoto-u.ac.jp/>, last access: 18 November 2022, World Data Center for Geomagnetism, Kyoto, 2022). The comparative analysis (Fig. 9) also shows that the geomagnetic components have a good correlation with Dst and ap indices, especially H and Dst. It should be noted that the H component in Fig. 9 has eliminated periodic changes such as secular variation and seasonal variation.

We compared the FTD outliers with the ap and Dst indices trying to establish the cause of the FTD out of tolerance, and took corresponding measures: (a) When the ap is greater than or equal to 24 nT, or Dst is less -30 nT, the outlier was considered to be caused by geomagnetic activity. The AHMVs at the corresponding time were not corrected. (b) When the ap is less than 24 nT and Dst is greater than -30 nT, we carefully looked for the cause of each FTD outlier by comparing the daily variation curves of multiple observatories (Sheshan, Chongming, Wuhan, Guangzhou, or Nanjing), and further consult the available documentation (*Observatory Communication Journal*, *Geomagnetic Observation Report*, *Chronicles of China Geomagnetic Observa-*

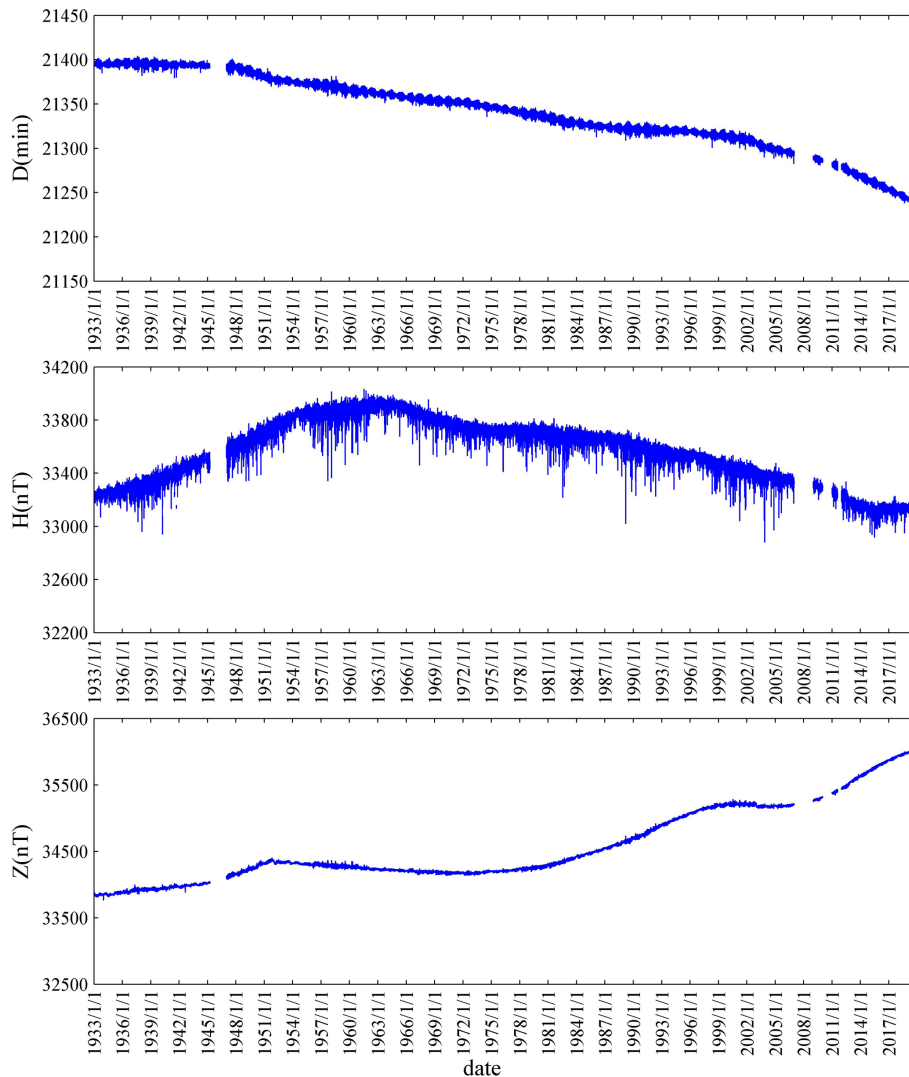


Figure 5. The AHMV plots of D , H , and Z components for all time from 1933 to 2019.

tory, and postal letters). A preliminary analysis found that for the D component, 65.6 % of the outliers were related to geomagnetic disturbance; the 33.5 % showed that no abnormality was found in the daily change curve; the remaining 82 values were questionable. For the H component, 80.5 % of the outliers were related to geomagnetic disturbance; the 17.6 % showed that no abnormality was found in the daily change curve; the remaining 199 values were questionable. For the Z component, 99.6 % of the outliers were related to geomagnetic disturbance; the 0.4 % showed that no abnormality was found in the daily change curve; the remaining 112 values were questionable. A total of 393 FTD outliers were questionable and no relevant and useful information was recorded in the available documentation. The AHMVs at the corresponding time were not corrected but were marked as questionable data in the datasets, the quality flag was $QC = Q$. As shown in Fig. 10, taking the FTD outliers of

19 October 2013 as an example, a clear deviation was found in the data between 08:00 to 13:00 from the real geomagnetic characteristics. Due to the lack of complete documentation, the questionable data were not corrected, just made the marks in the datasets, $QC = Q$. (c) When the ap index is less than 24 nT and Dst is greater than -30 nT, a change is registered in the available documentation. These data can be accepted to be corrected. In Table 2, we listed the date of the data to be corrected and the reasons recorded in the daily log and annual report. It took place only on 1 January 2003, a modern absolute instrument named Fluxgate Theodolite DIM-100 replaced the geomagnetic induction instrument Schulze, and an Overhauser Effect Proton Precession Magnetometer GSM-19F replaced the Proton Precession Magnetometer CZM-2. These changes led to sudden steps in size of about 1.9', 8, 40, and 35 nT in D , H , Z , and F components, respectively. The log recorded the exact jumps in the measurements dur-

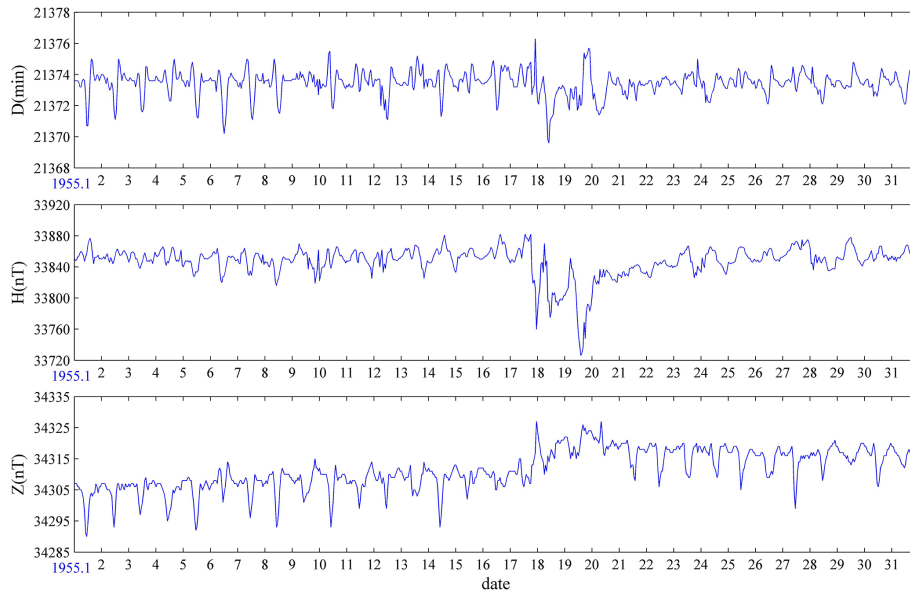


Figure 6. The AHMV record of January 1955 at SSH.

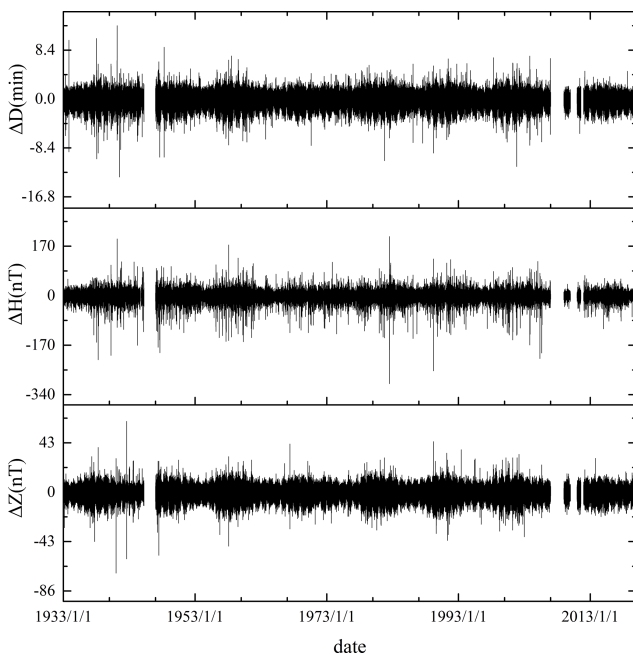


Figure 7. The FTD plots of D , H , and Z components.

ing the change of instruments at that time (SSH observatory, 2004).

4 Correction of the data problems

As was mentioned above, we only corrected the data of D , H , Z , and F components that occurred after 1 January 2003. The break arose due to the installation of new instruments in

1 January 2003. The corrected value is $1.9'$ for the D component, 8 nT for the H component, 40 nT for the Z component, and 35 nT for F component (see Table 2). As shown in Figs. 11 and 12, we gave the hourly and daily mean values curve of the D , H , and Z components before and after correction from 1 January 2001 to 31 December 2004. It can be seen that the quality of data has been greatly improved after correction.

The curve of the AHMVs shows obvious annual and seasonal variations. The seasonal variation shows that the variation range is large in summer and small in winter. The absolute daily mean value (ADMV) curve of the D component shows an obvious long-term trend of slow decline from 2001 to 2004. No obvious change characteristics can be seen in the Z curve.

Mutual comparison is an important method to check data quality. In general, the difference of the same component between two stations close to each other is small and stable. We also compared the data of the SSH before and after correction with those data from the Chongming Geomagnetic Observatory (IAGA code COM), which is the nearest observatory from the SSH (Fig. 13). The differences of the three components before correction are as follows: ΔD varies between -1.0 and 2.4 min, ΔH varies between -2 and 14 nT, and ΔZ varies between -46 and 19 nT. The differences of the three components after correction are as follows: ΔD varies between -0.3 and 1.3 min, ΔH varies between -7 and 24 nT, and ΔZ varies between -20 and 4 nT. The standard deviations of the differences of the three components before correction are as follows: 1.1 min, 3 nT, and 20 nT. The standard deviations of the differences of the three components after correction are as follows: 0.3 min, 3 nT and

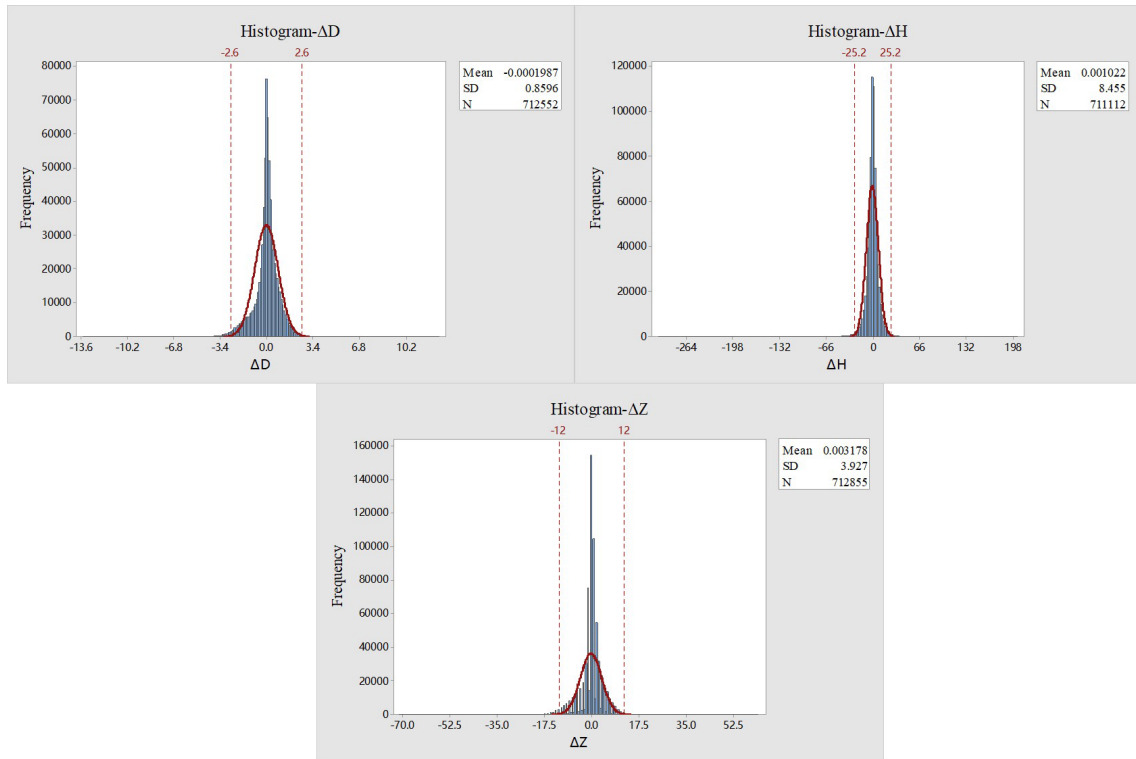


Figure 8. The histogram of the FTD of between 1933 and 2019.

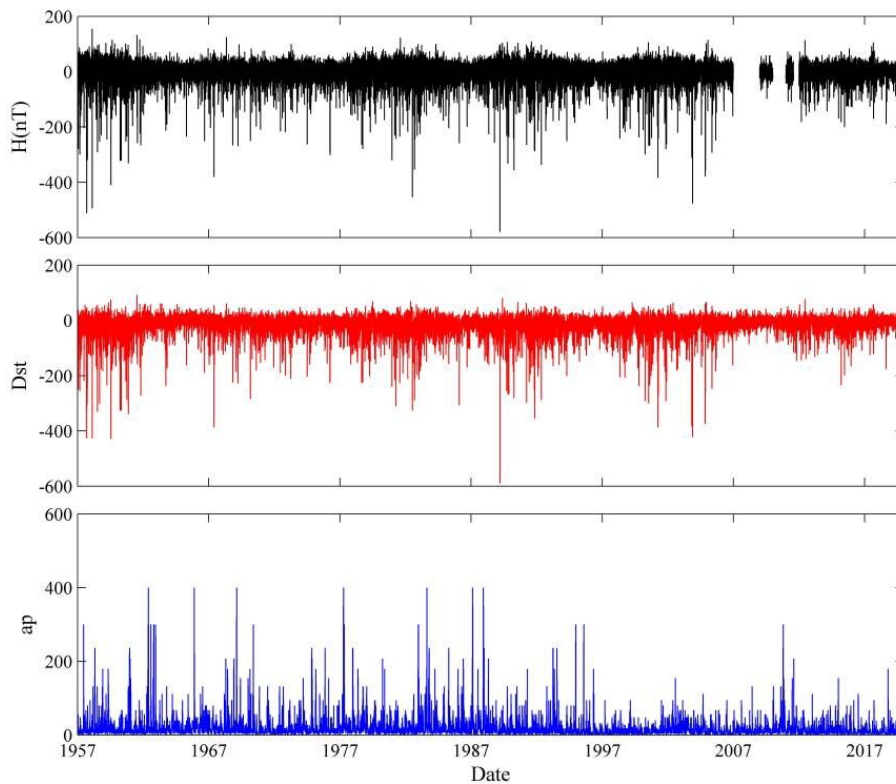


Figure 9. Comparative analysis of the H components with Dst and ap indices.

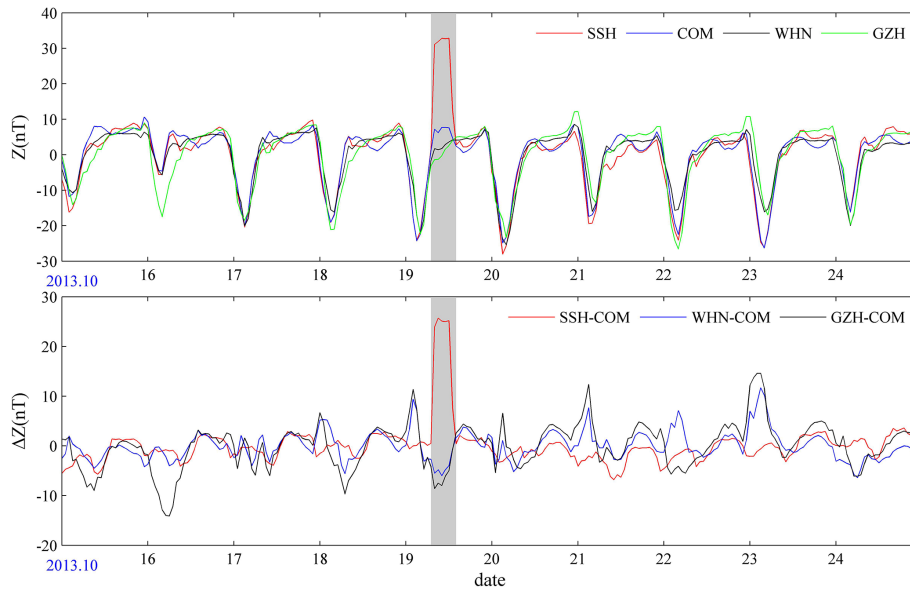


Figure 10. The contrast curve of SSH, COM, WHN, and GZH from 15 to 24 October 2013.

Table 2. Date and the reasons recorded of the data to be corrected.

| Date | Metadata | Time interval | Correction values (new values – old values) |
|----------------|-------------------------|---------------------------------|---|
| 1 January 2003 | Instrument replacements | 1 January 2003–31 December 2019 | D : 1.9' H : 8 nT Z : 40 nT F : 35 nT |

3.3 nT. Again, it shows that the quality of observation data is improved after correction.

5 Validation of the corrected series by compare with reference series

Intercomparison of time series for geomagnetic elements from adjacent observatories or geomagnetic models is also an important method to test accuracy and stability of data (Curto and Marsal., 2007). Firstly, we compared the rescued data with those data from the reference observatory. In China, the regular observation of most geomagnetic observatories began in the 1980s. Only eight geomagnetic observatories were established during the international geophysical year (Rasson et al., 2011). Among the eight observatories, the Guangzhou observatory (GZH) is closer to the Sheshan observatory. It started observation early, and the quality of observation data was good. So, we selected the GZH as the reference observatory. The GZH is located in Guangzhou City, Guangdong Province, about 1240 km northeast of the SSH. It began geomagnetic observation in 1957. Due to the interference of Guangzhou metro operation, the new site, Gaoyao Liantang Town, was selected in 1996. The construction of the new observatory was completed at the end of 2001. The geomagnetic observation records officially began in the new place on 1 January 2002.

We used GDPST which offers very useful diagnostic procedures of the data quality to plot intercomparison of the value curve and their difference curve from the SSH and GZH observatories on hourly and daily timescales to detect data with potential quality issues year by year. As an example, we presented AHMVs, ADMVs and their difference curves of the SSH and COM observatories in Fig. 14. At Fig. 14 in the upper panel (a), the AHMV and their difference curves are depicted, while in the lower panel (b), the ADMVs and their difference curves are plotted. On hourly scales, the single components D , H , and Z of the SSH and GZH behave roughly identical, and their difference series slowly fluctuates (due to geomagnetic activity) around a certain range. Spikes are caused in most cases by external disturbances. On daily timescales, the components D , H , and Z are roughly identical, but their differences clearly coincide with the variation of the geomagnetic field. It is because the distance between the two observatories are too far to completely offset the influence of internal and external source fields in different regions.

Comparing the measured values with the calculated values of the model for a long-time scale is not only an important means to check the stability of secular variation, but also an important means to evaluate the accuracy of the model (Zhang et al., 2008b; Chen et al., 2012). One of the aims of geomagnetic observatories is the monitoring of SV (Reda et al., 2011). Secondly, to monitor the SV of SSH, we compared

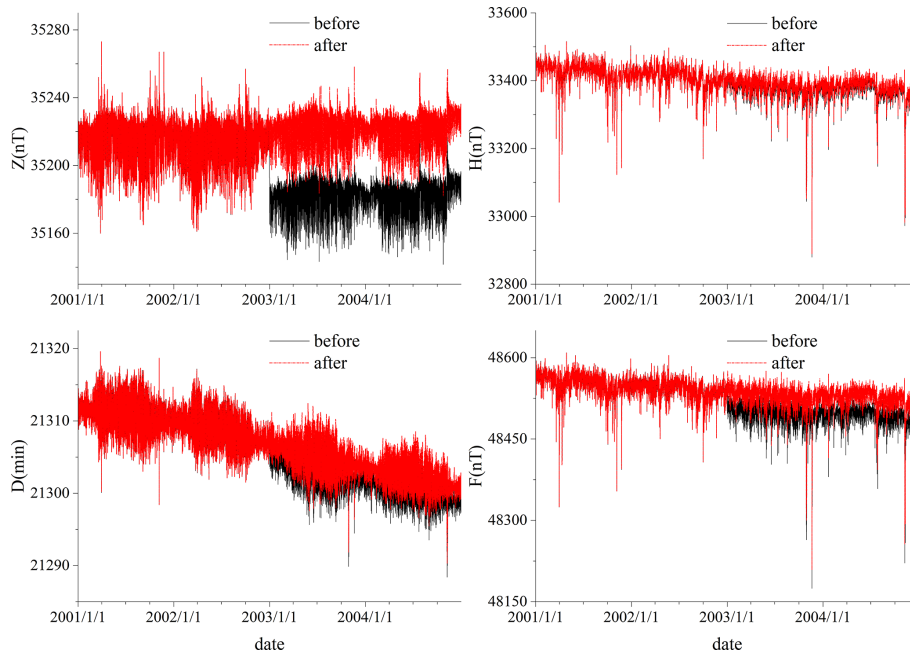


Figure 11. Plot of hourly mean values before and after correction.

the series curve of the annual mean values (AMVs) for the X , Y , and Z components calculated from the rescued records with these data calculated from the COV-OBS model (Gillet et al., 2013; Huder et al., 2020). The COV-OBS.x2 model covers the period from 1840 to 2020. The data source of the model is from observatory data, satellite data, and the older surveys. The model can give the field contributions from the internal and external sources.

As can be seen from the Fig. 15, the change trends of X , Y , and Z components from the SSH and COV-OBS model are very consistent. The X component increased year by year before 1962 and generally decreased after 1962; from 1933 to 2019, the Y component shows a general downward trend and the Z component shows a general upward trend. There are differences between AMVs of the SSH and these data calculated from the COV-OBS model, the X component varies from -210 to -276 nT, the Y component varies from 17 to 94 nT, and the Z component varies from 198 to 289 nT. According to the preliminary analysis, the main reasons for the large difference between the SSH and COV-OBS model may be the local magnetic anomaly in the Sheshan area, the uneven distribution of global stations, the lack of modeling data, and data-quality problems in the SSH. This fully illustrates the importance of continuous and high-quality data in magnetic field modeling.

6 Application examples of SSH datasets

We calculated the first-time derivative (FTD) using a difference between 2 consecutive years as SV and plotted the SV

from the rescued data and COV-OBS model to detect possible geomagnetic jerks over the past 90 years. For all geomagnetic components, the SV is calculated as

$$dX/dt(\text{year}) = (X(\text{year}) - X(\text{year} - 1))/1, \quad (3)$$

where X denotes the geomagnetic field components D , H , and Z .

Geomagnetic jerks are defined as V-like or Λ -like changes in the SV and occur in a time period of a few months (Courtillot and Le Mouél, 1984; Morozova et al., 2014; Kang et al., 2020). “The geomagnetic jerks are due to interactions of the core field and the rapid time-varying core flow” (Kuang and Tangborn, 2011). Since Malin and Hodder (1982), Courtillot and Le Mouél (1984) discovered the geomagnetic jerk in 1969, 10 jerks have been detected in observatories from 1933 to 2020, of which 1969, 1978 (Alexandrescu et al., 1996), 1991 (De Michelis et al., 1998), 1999 (Mandea et al., 2000; Zhang et al., 2008a), 2003 (Mandea and Olsen, 2007; Feng et al., 2018; He et al., 2019), 2007 (Kotzé, 2010; Chulliat et al., 2010), and 2014 (Brown et al., 2016; Kloss and Finlay, 2019; Finlay et al., 2016; Kang et al., 2020) were global events. In addition, there were two local events which occurred in 1949 (Mandea et al., 2000) and 2011 (Chulliat and Maus, 2014; Kotzé and Korte, 2016). In 2017, there were similar characteristics of geomagnetic jerks, which may be a new geomagnetic jerk (He et al., 2019; Pavón-Carrasco et al., 2021). The jerks are more easily seen in the eastward component (Y) of the geomagnetic secular variation. Not all jerks can be detected around the world, some seem to be seen only in limited regions (Morozova et al., 2014), and its occurrence time is not exactly the same at each observatory.

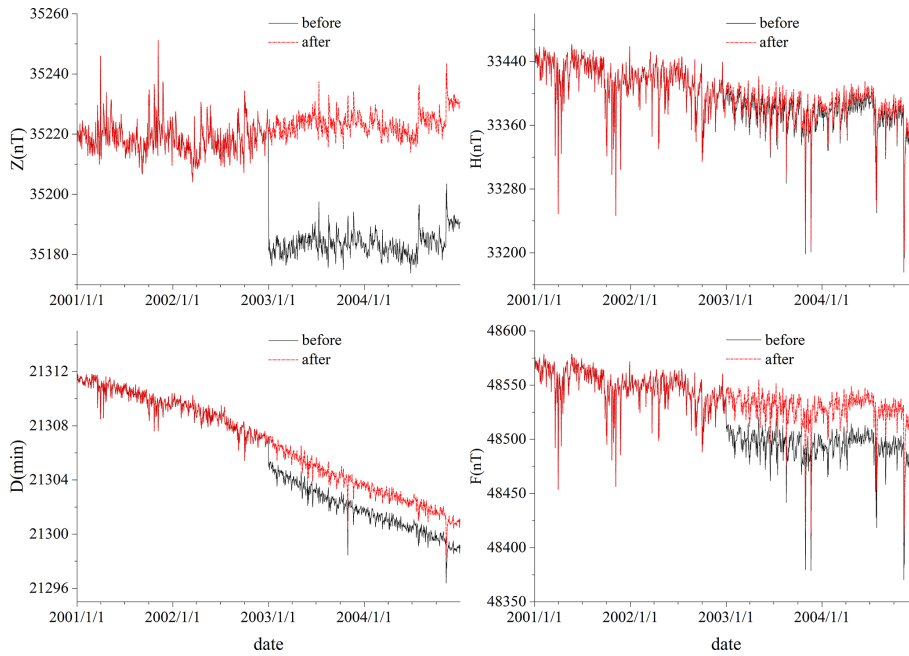


Figure 12. Plot of daily mean values before and after correction.

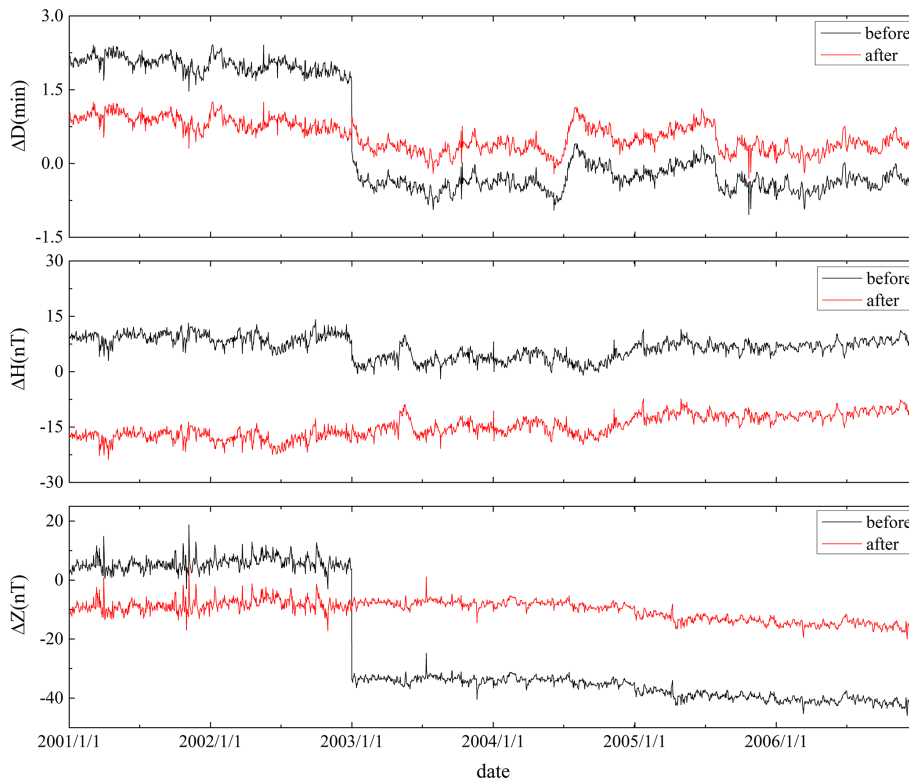


Figure 13. Plot of difference between the SSH and COM before and after correction.

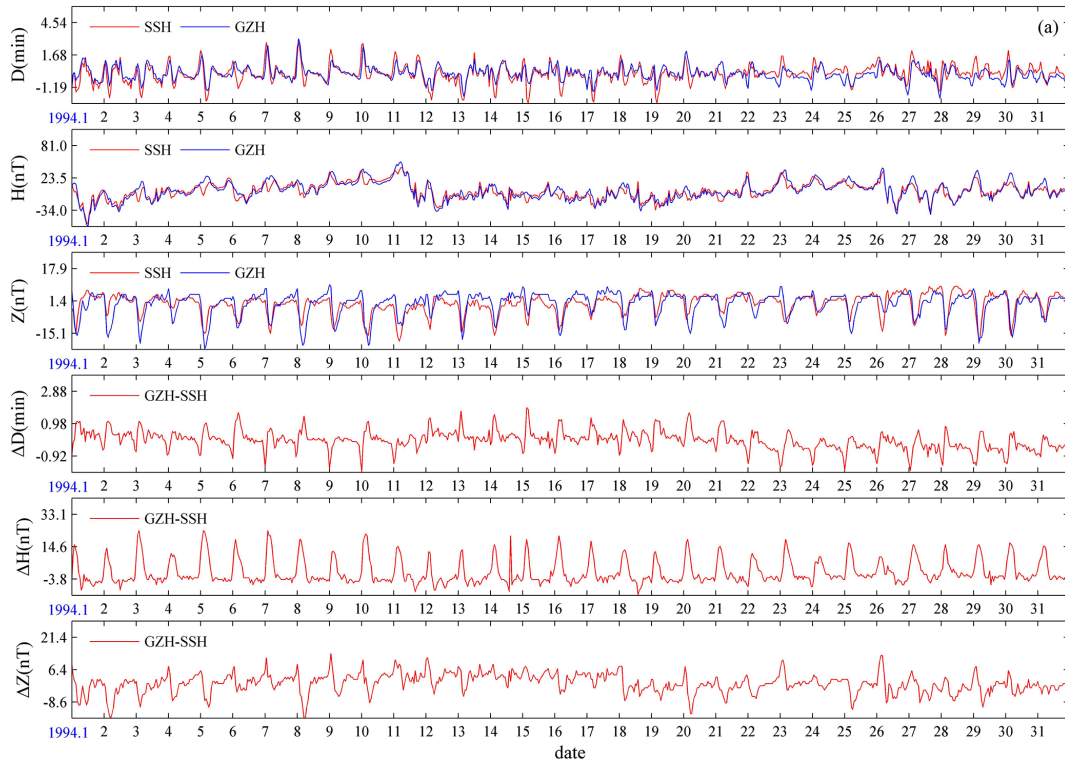


Figure 14.

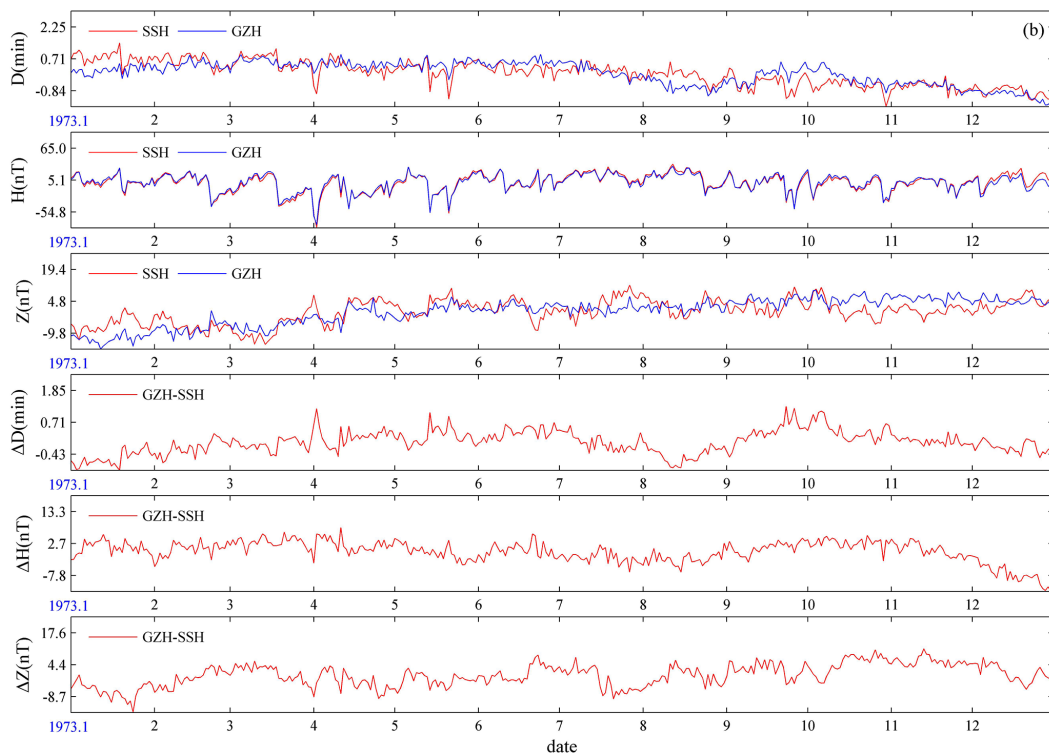


Figure 14. AHMVs, ADMVs and their difference curves of the SSH and GZH observatories. (a) AHMVs and their difference curves. (b) ADMVs and their difference curves.

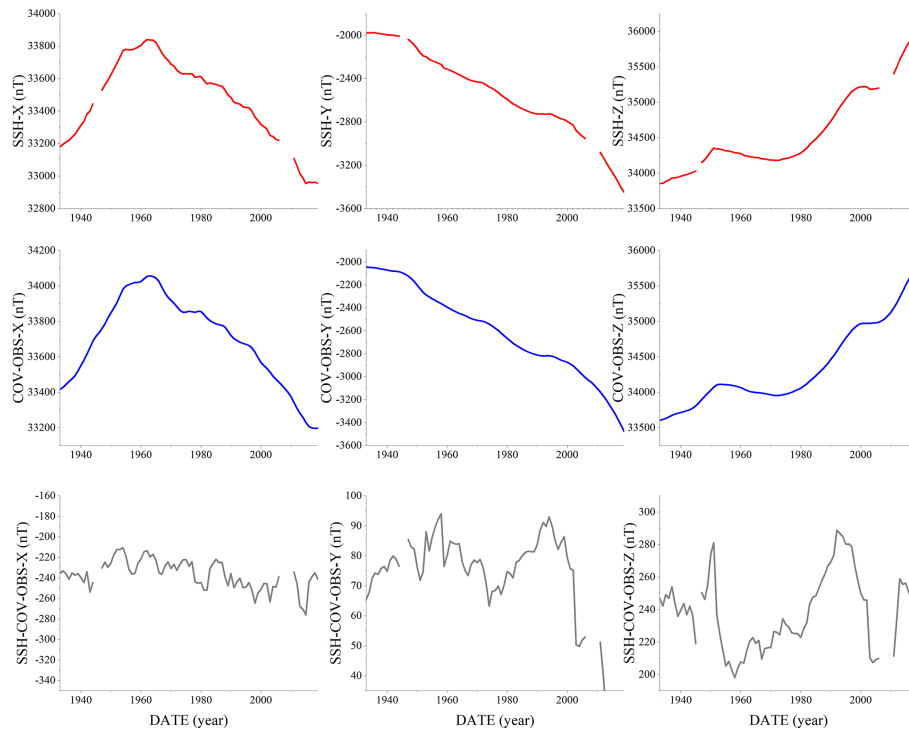


Figure 15. The AMV and their difference curves of X, Y, Z components calculated from the rescued records and the COV-OBS model.

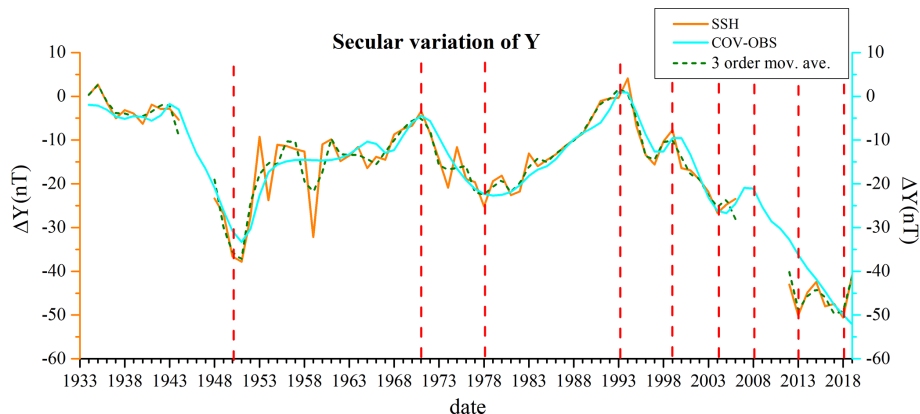


Figure 16. The SV of the annual Y series from the SSH and COV-OBS model.

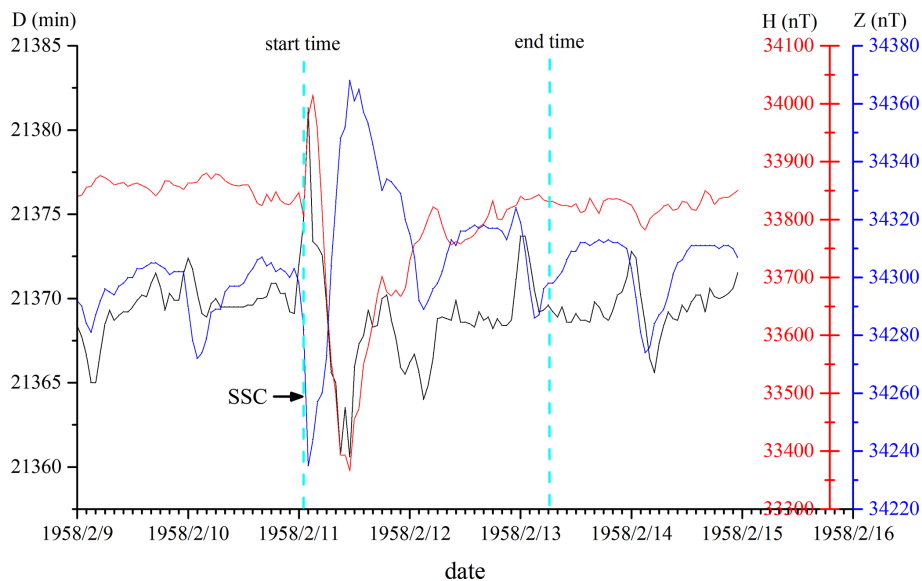
Figure 16 gives the SV of the annual Y series from the SSH and COV-OBS model, and the dotted blue line is the third-order moving average curve of the Y component SV at the SSH. Nine jerks are clearly seen in the plot. They occurred in 1950, 1971, 1978, 1993, 1999, 2004, 2008, 2013, and 2018. Except for the jerks that occurred in 1978 and 1999, other events were a little later as seen at the SSH. Between 2008 and 2017, only one jerk (in 2013) is seen at the SSH, which is inconsistent with the study of other scholars mentioned above. They observed jerk events in 2011 and 2014, respectively. We cannot see a potential jerk in 2011, maybe because of the data gap until 2011.

A geomagnetic storm is a global phenomenon of magnetic disturbance. At low and mid-latitudes, it mainly manifests itself as a decrease in the horizontal geomagnetic field (H) during a geomagnetic storm. According to the Kakioka Magnetic Observatory Website (2022), a total of 67 very large geomagnetic storms (variation range of the H component >300 nT) have occurred since 1933. Referring to the start and end time of the geomagnetic storm announced by the website, we studied the geomagnetic storms that were recorded in the data series of the SSH since 1933. We found a total of 42 very large geomagnetic storms (variation range of the H component >300 nT) in these data se-

Table 3. List of geomagnetic storms that have occurred at the SSH since 1933.

| SN | Start time | End time | Variation amplitude | | | SN | Start time | End time | Variation amplitude | | |
|----|-------------------------|-------------------------|---------------------|-----|-----|----|-------------------------|-------------------------|---------------------|-----|-----|
| | | | H | D | Z | | | | H | D | Z |
| 1 | 22 August 1937 03:00 | 23 August 1937 15:00 | 329 | 157 | 82 | 22 | 27 August 1978 02:00 | 31 August 1978 20:00 | 312 | 104 | 55 |
| 2 | 22 January 1938 02:00 | 23 January 1938 24:00 | 366 | 113 | 40 | 23 | 13 July 1982 16:00 | C | 538 | 156 | 56 |
| 3 | 25 January 1938 11:00 | 27 January 1938 10:00 | 333 | 160 | 39 | 24 | 5 September 1982 22:00 | 8 September 1982 02:00 | 385 | 148 | 68 |
| 4 | 24 March 1940 13:00 | 26 March 1940 08:00 | 534 | 109 | 76 | 25 | 21 September 1982 03:00 | 23 September 1982 21:00 | 306 | 100 | 61 |
| 5 | 2 March 1947 08:00 | 4 March 1947 22:00 | 338 | 74 | 68 | 26 | 4 February 1983 16:00 | 6 February 1983 20:00 | 303 | 88 | 33 |
| 6 | 24 January 1949 18:00 | C | 333 | 127 | 53 | 27 | 6 February 1986 13:00 | 10 February 1986 03:00 | 328 | 162 | 36 |
| 7 | 12 May 1949 06:00 | 15 May 1949 18:00 | 431 | 113 | 87 | 28 | 13 March 1989 01:00 | 15 March 1989 22:00 | 629 | 185 | 114 |
| 8 | 19 March 1950 05:00 | 19 March 1950 23:00 | 383 | 135 | 84 | 29 | 20 October 1989 09:00 | 23 October 1989 10:00 | 318 | 96 | 63 |
| 9 | 13 September 1957 00:00 | 14 September 1957 16:00 | 557 | 152 | 112 | 30 | 9 April 1990 08:00 | 11 April 1990 24:00 | 388 | 94 | 73 |
| 10 | 29 September 1957 00:00 | 2 October 1957 10:00 | 384 | 118 | 86 | 31 | 8 November 1991 06:00 | 10 November 1991 03:00 | 326 | 163 | 54 |
| 11 | 11 February 1958 01:00 | 13 February 1958 06:00 | 649 | 210 | 133 | 32 | 9 May 1992 19:00 | 12 May 1992 07:00 | 434 | 116 | 80 |
| 12 | 8 July 1958 07:00 | 10 July 1958 11:00 | 386 | 126 | 96 | 33 | 6 April 2000 16:00 | 7 April 2000 20:00 | 321 | 130 | 53 |
| 13 | 3 September 1958 08:00 | 6 September 1958 13:00 | 306 | 107 | 65 | 34 | 15 July 2000 14:00 | 16 July 2000 18:00 | 317 | 130 | 68 |
| 14 | 15 July 1959 08:00 | 17 July 1959 02:00 | 488 | 150 | 115 | 35 | 31 March 2001 00:00 | 1 April 2001 15:00 | 447 | 175 | 97 |
| 15 | 31 March 1960 09:00 | 2 April 1960 23:00 | 332 | 126 | 106 | 36 | 24 November 2001 05:00 | 25 November 2001 24:00 | 317 | 87 | 78 |
| 16 | 30 April 1960 12:00 | 1 May 1960 20:00 | 364 | 97 | 82 | 37 | 29 October 2003 06:00 | C | 330 | 160 | 50 |
| 17 | 12 November 1960 13:00 | 14 November 1960 23:00 | 387 | 140 | 49 | 38 | 30 October 2003 16:00 | 2 November 2003 21:00 | 323 | 140 | 42 |
| 18 | 30 September 1961 21:00 | 1 October 1961 20:00 | 340 | 47 | 33 | 39 | 20 November 2003 08:00 | 21 November 2003 24:00 | 461 | 100 | 39 |
| 19 | 25 May 1967 12:00 | 29 May 1967 20:00 | 459 | 116 | 80 | 40 | 7 November 2004 18:00 | C | 453 | 120 | 34 |
| 20 | 23 March 1969 18:00 | 25 March 1969 24:00 | 303 | 95 | 64 | 41 | 9 November 2004 18:00 | 12 November 2004 24:00 | 343 | 123 | 39 |
| 21 | 25 March 1976 13:00 | 27 March 1976 24:00 | 333 | 93 | 53 | 42 | 15 May 2005 02:00 | 16 May 2005 18:00 | 378 | 98 | 30 |

Note C in “End time”: followed by another storm.

**Figure 17.** The geomagnetic storm occurred on 11 February 1958.

ries (Table 3). Figure 17 shows an example of a very large geomagnetic storm that occurred on 11 February 1958. A sudden storm commencement (SSC) occurred at 01:00 on 11 February 1958. It is the sign of the start of the geomagnetic storm. This storm lasted about 53 h and ended at 06:00 on the 13 February 1958. The maximum variation amplitude of D , H and Z during the geomagnetic storm is 210, 649 and 133 nT respectively.

7 Data availability

The digitized and quality-controlled absolute hourly mean value (AHMV) data are available at: <https://doi.org/10.5281/zenodo.7005471> (Zhang et al., 2022). The data are provided in Microsoft Excel format, including the observed AHMV files of the three components (D , H and Z) at the SSH for 1933–2019, and also the metadata files about the datasets.

8 Conclusion

This paper presents the acquisition process, quality control, data correction, quality examination, and application examples of the datasets of the SSH from 1933 to 2019. The quality examination results show that the corrected data have a good agreement with the reference observatory data and the model data. This fully indicates that the rescued data are of good quality. The datasets are valuable for studying the geomagnetic daily variation, geomagnetic field model construction, and secular variation. It should be noted that the data marked with Q ($QC = Q$) are used with caution for the reasons mentioned above. A few problems were found in the acquisition of geomagnetic historical datasets: (1) the rescue of paper data is a time-consuming and laborious work. For example, the font color of some reports is light, which makes automatic recognition difficult. We can only recognize and input by key. (2) Some metadata of the SSH has been missing, which brings difficulties to the identification and correction of data. Therefore, we believe that we should do our best to rescue historical data to avoid the irreparable losses over time. Our plan for the next phase is to rescue the historical data from 1874 to 1932 at SSH, as well as from other observatories, to provide more high-quality data for the geomagnetic science community.

Author contributions. SZ performed data correction, quality assessment, and the analysis of application example. SZ prepared the manuscript. CF calculated the X , Y , and Z components from the COV-OBS model, drew pictures, and performed revision of the manuscript. GZ was responsible for the digitization of paper data from 1933 to 1945 of the SSH and provided digital series of the geomagnetic components of 2009 and 2011. CC designed a set of Excel templates. JW developed the data import software. SH and PG collected and organized metadata. GC sorted out the geomagnetic storm list and geomagnetic indices.

Competing interests. The contact author has declared that none of the authors has any competing interests.

Disclaimer. Publisher's note: Copernicus Publications remains neutral with regard to jurisdictional claims in published maps and institutional affiliations.

Acknowledgements. We thank SSH, GNC, and the reference room of the Institute of Geophysics, China Earthquake Administration for providing the valuable data resources. We are grateful to editors and anonymous reviewers for their helpful reviews. We sincerely thank all the staff who have ever worked or are currently working at the SSH. We also thank GeoForschung Zentrum Potsdam, Germany, for providing online ap indices, World Data Center for Geomagnetism, Kyoto, for providing online Dst indices,

and the Kakioka Magnetic Observatory of the Japan Meteorological Agency for providing the online magnetic storm catalog.

Financial support. This work was funded by the National Key R&D Program of China (grant no. 2017YFC1500205), the National Natural Science of Foundation of China (grant no. 41974073), the Macau Foundation, and the pre-research project of Civil Aerospace Technologies of China (grant no. D020308).

Review statement. This paper was edited by Kirsten Elger and reviewed by two anonymous referees.

References

- Alexandrescu, M., Gibert, D., Hulot, G., Le Mouél, J. L., and Saracco, G.: Worldwide wavelet analysis of geomagnetic jerks, *J. Geophys. Res.*, 101, 21975–21994, 1996.
- Bolduc, L., Langlois, P., Boteler, D., and Pierre.: A study of geomagnetic disturbance in Quebec. I. General results, *IEEE T. Power Deliver.*, 13, 1251–1256, 1998.
- Bolduc, L., Langlois, P., Boteler, D., and Pirjola, R.: A study of geoelectromagnetic disturbances in quebec. II. Detailed analysis of a large event, *IEEE T. Power Deliver.*, 15, 272–278, 2002.
- Boteler, D. H., Pirjola, R. J., and Nevanlinna, H.: The effects of geomagnetic disturbances on electrical systems at the Earth's surface, *Adv. Space Res.*, 22, 17–27, 1998.
- Brown, W., Beggan, C., and Macmillan, S.: Geomagnetic jerks in the Swarm Era, Proceedings of the ESA Living Planet Symposium, Prague, Czech Republic, 9–13 May 2016, <https://nora.nerc.ac.uk/id/eprint/514296/> (last access: 18 November 2022), 2016.
- Capozzi, V., Cotroneo, Y., Castagno, P., De Vivo, C., and Budillon, G.: Rescue and quality control of sub-daily meteorological data collected at Montevergine Observatory (Southern Apennines), 1884–1963, *Earth Syst. Sci. Data*, 12, 1467–1487, <https://doi.org/10.5194/essd-12-1467-2020>, 2020.
- Chen, B., Gu, Z. W., Gao, J. T., Yuan, J. H., and Di, C. Z.: Geomagnetic secular variation in China during 2005–2010 described by IGRF-11 and its error analysis, *Progress in Geophysics*, 27, 512–521, 2012 (in Chinese).
- Chen, J., Jiang, Y. L., Zhang, X. X., Chen, C. H., Yang D. M., and Liu H. F.: The design of HVDC discrimination and processing system for geomagnetic network, *Seismological and Geomagnetic Observation and Research*, 35, 271–274, 2014 (in Chinese).
- Chulliat, A. and Maus, S.: Geomagnetic secular acceleration, jerks, and a localized standing wave at the core surface from 2000 to 2010, *J. Geophys. Res.*, 119, 1531–1543, 2014.
- Chulliat, A., Peltier, A., Truong, F., and Fouassier, D.: Proposal for a new observatory data product: quasi-definitive data, 11th IAGA Scientific Assembly, Sopron, Hungary, 23–30 August 2009, Abstract Book, 94 pp., 2009.
- Chulliat, A., Thébault, E., and Hulot, G.: Core field acceleration pulse as a common cause of the 2003 and 2007 geomagnetic jerks, *Geophys. Res. Lett.*, 37, L07301, <https://doi.org/10.1029/2009GL042019>, 2010.
- Clarke, E., Flower, S., Humphries, T., McIntosh, R., McTaggart, F., McIntyre, B., Owenson, N., Henderson, K., Mann, E., MacKen-

- zie, K., Piper, S., Wilson, L., and Gillanders, R.: The digitization of observatory magnetograms, poster presented at: 11th IAGA Scientific Assembly, Sopron, Hungary, 23–30 August 2009, <https://www.osti.gov/etdeweb/biblio/21389614> (last access: 18 November 2022), 2009.
- Courtillot, V. and Le Mouél, J. L.: Geomagnetic secular variation impulses, *Nature*, 311, 709–716, 1984.
- Curto, J. J. and Marsal, S.: Quality control of Ebro magnetic observatory using momentary values, *Earth Planets Space*, 59, 1187–1196, 2007.
- Dawson, E., Reay, S., Macmillan, S., Flower, S., and Shanahan, T.: Quality control procedures at the World Data Centre for Geomagnetism (Edinburgh), IAGA 11th Scientific Assembly, Sopron, Hungary, 23–30 August 2009, https://www.researchgate.net/publication/264590163_Quality_control_procedures_at_the_World_Data_Centre_for_Geomagnetism_Edinburgh (last access: 18 November 2022), 2009.
- De Michelis, P., Cafarella, L., and Meloni, A.: Worldwide character of the 1991 geomagnetic jerk, *Geophys. Res. Lett.*, 25, 377–380, 1998.
- Department of science, technology and monitoring, CEA: The Chronicles of China Geomagnetic Observatory, 1984 (in Chinese).
- Dong, X. H., Li, X. J., Zhang, G. Q., Shi, J., and Liu, C.: The study of digital identification of magnetogram, *Seismological and Geomagnetic Observation and Research*, 30, 49–55, 2009 (in Chinese).
- Feng, Y., Holme, R., Cox, G. A., and Jiang, Y.: The geomagnetic jerk of 2003.5: Characterisation with regional observatory secular variation data, *Phys. Earth Planet. In.*, 278, 47–58, 2018.
- Finlay, C. C., Olsen, N., Kotsiaros, S., Gillet, N., and Tøffner-Clausen, L.: Recent geomagnetic secular variation from *Swarm* and ground observatories as estimated in the CHAOS-6 geomagnetic field model, *Earth Planets Space*, 68, 112, <https://doi.org/10.1186/s40623-016-0486-1>, 2016.
- Gao, M. Q. and Hu, Z. Y.: Establishment of historical data and database of rescue Sheshan observatory, in: Proceedings of the 9th Annual Academic Meeting of China Geophysical Society, Beijing, China, September 1993, 262, <https://cpfd.cnki.com.cn/Article/CPFDTOTAL-ZGDW199309001262.htm> (last access: 18 November 2022), 1993 (in Chinese).
- GeoForschung Zentrum Potsdam Website: Kp and ap values, <https://www.gfz-potsdam.de/en/section/geomagnetism/data-products-services/>, last access: 18 November 2022.
- Gillet, N., Jault, D., Finlay, C. C., and Olsen, N.: Stochastic modeling of the Earth's magnetic field: Inversion for covariances over the observatory era, *Geochem. Geophys. Geosy.*, 14, 766–786, 2013.
- Guo, S. X., Liu, L. G., Pirjola, R. J., and Wang, K. R., and Dong, B.: Impact of EHV power system on geomagnetically induced currents in UHV power system, *IEEE T. Power Deliver.*, 30, 2163–2170, 2015.
- He, Y. F., Zhao, X. D., Zhang, S. Q., Yang, D. M., and Li, Q.: Geomagnetic jerks based on the midnight mean of the geomagnetic field from geomagnetic networks of China, *Acta Seismologica Sinica*, 41, 512–523, <https://doi.org/10.11939/jass.20190009>, 2019 (in Chinese).
- Huder, L., Gillet, N., Finlay, C., Hammer, M., and Hervé Tchoungui.: COV-OBS.x2: 180 years of geomagnetic field evolution from ground-based and satellite observations, *Earth Planets Space*, 72, 160, <https://doi.org/10.1186/s40623-020-01194-2>, 2020.
- Institute of Geophysics, Chinese Academy of Sciences: Geomagnetic Observation Report, 1965 (in Chinese).
- Kakioka Magnetic Observatory Website: Geomagnetic Storm Catalog, <https://www.kakioka-jma.go.jp/en/index.html>, last access: 18 August 2022.
- Kang, G. F., Gao, G. M., Wen, L. M., and Bai, C. H.: The 2014 geomagnetic jerk observed by geomagnetic observatories in China, *Chinese Journal of Geophysics*, 63, 4144–4153, <https://doi.org/10.6038/cjg2020N0337>, 2020 (in Chinese).
- Kappenman, J. G.: Geomagnetic storms and their impact on power systems, *IEEE Power Engineering Review*, 16, 5–8, 1996.
- Kloss, C. and Finlay, C. C.: Time-dependent low-latitude core flow and geomagnetic field acceleration pulses, *Geophys. J. Int.*, 217.1, 140–168, <https://doi.org/10.1093/gji/ggy545>, 2019.
- Korte, M., Manda, M., Linthe, H. J., Hemshorn, A., Kotzé, P., and Ricaldi, E.: New geomagnetic field observations in the South Atlantic Anomaly region, *Ann. Geophys.*, 52, 65–81, 2009.
- Kotzé, P. B.: The 2007 geomagnetic jerk as observed at the Hermanus magnetic observatory, *Phys. Comment.*, 2, 5–6, 2010.
- Kotzé, P. B. and Korte, M.: Morphology of the southern African geomagnetic field derived from observatory and repeat station survey observations: 2005–2014, *Earth Planets Space*, 68, 23, <https://doi.org/10.1186/s40623-016-0403-7>, 2016.
- Kuang, W. J. and Tangborn, A.: Interpretation of Core Field Models, in: *Geomagnetic Observations and Models*, vol. 5, edited by: Manda, M. and Korte, M., Springer Science + Business Media, 295–309, eBook ISBN 978-90-481-9858-0, 2011.
- Linthe, H. J., Reda, J., Isac, A., Matzka, J., and Turbitt, C.: Observatory data quality control-the instrument to ensure valuable research, in: Proceedings of the XVth IAGA Workshop on Geomagnetic Observatory Instruments, Data Acquisition and Processing: extended abstract volume, edited by: Hejda, P., San Fernando, Spain, March 2013, 173–177, <https://core.ac.uk/download/pdf/20319986.pdf> (last access: 18 November 2022), 2013.
- Liu, C. M., Liu, L. G., and Pirjola, R.: Geomagnetically induced currents in the high voltage power grid in China, *IEEE T. Power Deliver.*, 24, 2368–2374, 2009.
- Liu, L. G., Liu, C. M., Zhang, B., Wang, Z. Z., Xiao, X. N., and Han, L. Z.: Strong magnetic storm's influence on China's Guangdong power grid, *Chinese Journal of Geophysics*, 51, 976–981, <https://doi.org/10.3321/j.issn:0001-5733.2008.04.004>, 2008 (in Chinese).
- Liu, L. G., Ge, X. N., Wang, K. R., Zong, W., and Liu C. M.: Observation studies of encroachment by geomagnetic storms on high-speed railways and oil-and-gas pipelines in China, *Sci. Sin. Tech.*, 46, 268–275, <https://doi.org/10.1360/N092015-00279>, 2016 (in Chinese).
- Malin, S. R. C. and Hodder, B. M.: Was the 1970 geomagnetic jerk of internal or external origin?, *Nature*, 296, 726–728, 1982.
- Manda, M. and Olsen, N.: Investigation of a secular variation impulse using satellite data: The 2003 geomagnetic jerk, *Earth Planet. Sc. Lett.*, 255, 94–105, 2007.
- Manda, M., Bellanger, E., and Le Mouél, J. L.: A geomagnetic jerk for the end of the 20th century?, *Earth Planet. Sc. Lett.*, 183, 369–373, 2000.

- Menvielle, M., Iyemori, T., Marchaudon, A., and Nosé, M.: Geomagnetic indices, in: *Geomagnetic Observations and Models*, vol. 5, edited by: Manda, M. and Korte, M., Springer Science + Business Media, 127–148, eBook ISBN 978-90-481-9858-0, 2011.
- Mestre, O., Domonkos, P., Picard, F., Auer, I., Robin, S., Lebarbier, E., Böhm, R., Aguilar, E., Guijarro, J., Vertachnik, G., Klancar, M., Dubuisson, B., and Stepanek, P.: HOMER: a homogenization software – methods and applications, 117, 47–67, https://www.researchgate.net/publication/281471961_HOMER_A_homogenization_software_-_methods_and_applications (last access: 18 November 2022), 2013.
- Morozova, A. L., Ribeiro, P., and Pais, M. A.: Correction of artificial jumps in the historical geomagnetic measurements of Coimbra Observatory, Portugal, *Ann. Geophys.*, 32, 19–40, 2014.
- Morozova, A. L., Ribeiro, P., and Pais, M. A.: Homogenization of the historical series from the Coimbra Magnetic Observatory, Portugal, *Earth Syst. Sci. Data*, 13, 809–825, <https://doi.org/10.5194/essd-13-809-2021>, 2021.
- Pang, J. Y., Chen, J., Wang, C., Teng, Y. T., Zhao, Y. G., and Li, Z. G.: The principle of power interference and its automatic processing during geoelectrical resistivity observation, *Seismological and Geomagnetic Observation and Research*, 34, 117–122, 2013 (in Chinese).
- Pavón-Carrasco, F. J., Marsal, S., Campuzano, S. A., and Torta, M.: Signs of a new geomagnetic jerk between 2019 and 2020 from Swarm and observatory data, *Earth, Planets and Space*, 73, 175, <https://doi.org/10.1186/s40623-021-01504-2>, 2021.
- Peng, F., Shen, X., Tang, K., Zhang, J., Huang, Q., Xu, Y., Yue, B., and Yang, D.: Data-Sharing Work of the World Data Center for Geophysics, *Beijing Data Sci. J.*, 6, 404–407, 2007 (in Chinese).
- Rasson, J. L., Toh, H., and Yang D. M.: The Global Geomagnetic Observatory Network, in: *Geomagnetic Observations and Models*, vol. 5, edited by: Manda, M. and Korte, M., Springer Science + Business Media, 1–25, eBook ISBN 978-90-481-9858-0, 2011.
- Reay, S. J., Clarke, E., Dawson, E., and Macmillan, S.: Operations of the World Data Centre for Geomagnetism, Edinburgh, *Data Science Journal*, 12, WDS47–WDS51, 2013.
- Reda, J., Fouassier, D., Isac, A., Linthe, H. J., Matzka, J., and Turbitt, C. W.: Improvements in Geomagnetic Observatory Data Quality, in: *Geomagnetic Observations and Models*, vol. 5, edited by: Manda, M. and Korte, M., Springer Science + Business Media, 127–148, eBook ISBN 978-90-481-9858-0, 2011.
- Sergeyeva, N., Gvishiani, A., Soloviev, A., Zabarinskaya, L., Krylova, T., Nisilevich, M., and Krasnoperov, R.: Historical *K* index data collection of Soviet magnetic observatories, 1957–1992, *Earth Syst. Sci. Data*, 13, 1987–1999, <https://doi.org/10.5194/essd-13-1987-2021>, 2021.
- SSH observatory: Geomagnetic Observation Report of SSH observatory, 2004.
- Thomson, A. W. P.: Geomagnetism Review 2019, British Geological Survey Open Report, OR/20/00852, http://www.geomag.bgs.ac.uk/documents/reviews/Gomagnetism_Review_2019.pdf (last access: 18 November 2022), 2020.
- World Data Center for Geomagnetism, Kyoto: Dst values, <http://wdc.kugi.kyoto-u.ac.jp/>, last access: 18 November 2022.
- Xu, W. Y.: *Physics of Electromagnetic Phenomena of the Earth*, Hefei: University of Science and Technology of China press, 558 pages, ISBN 978-7312022562, 2009 (in Chinese).
- Zhang, S., Zhu, G., Wang, J., Chen, C., He, S., and Guo, P.: Quality-controlled geomagnetic hourly mean values datasets of Sheshan observatory from 1933 to 2019, Zenodo [data set], <https://doi.org/10.5281/zenodo.7005471>, 2022.
- Zhang, S. Q., Yang, D. M., Li, Q., and Zhao, Y. F.: The 1991 and 1999 jerks in China, *Earthquake Research in China*, 24, 253–260, 2008a (in Chinese).
- Zhang, S. Q., Yang, D. M., Li, Q., and Zhao, Y. F.: The consistence analysis of IGRF model value and annual mean value of some geomagnetic observatories in China, *Seismological and Geomagnetic Observation and Research*, 29, 42–29, 2008b (in Chinese).
- Zhang, S. Q., Fu, C. H., He, Y. F., Yang, D. M., Li, Q., Zhao, X. D., and Wang, J. J.: Quality Control of Observation Data by the Geomagnetic Network of China, *Data Science Journal*, 15, p. 15, <https://doi.org/10.5334/dsj-2016-015>, 2016.
- Zhao, X. D., He, Y. F., Chen, J., Zhang, S. Q., Li, Q., and Yuan, Y. R.: The distribution of ring current and field-aligned current during storms based on ground observatory data, *Chinese Journal of Geophysics*, 62, 3209–3222, <https://doi.org/10.6038/cjg2019M0268>, 2019 (in Chinese).
- Zhao, X. K., Wu, B. Y., and N., B. Q.: The geomagnetic dataset of Beijing Ming Tombs station (1991–2001), *China Scientific Data*, 2, 1–9, <https://www.docin.com/p-1982391171.html> (last access: 20 November 2022), 2017.